Nonlinear Stress-Strain and Strength Response of Axisymmetric Bimodulus Composite Material Shells

David W. Schmueser*
General Motors Research Laboratories, Warren, Michigan

Bimodulus materials are those which exhibit different material response when stressed in compression rather than tension. Strength predictions of laminated composites can be affected by bimodulus material response and nonlinear stress-strain behavior in individual laminae. Most applications of phenomenological failure models to laminated composites assume that lamina yield and ultimate lamina strength are the same. In addition, bimodulus material response is frequently neglected when applying failure models to predict laminate strength. This paper presents an investigation of the effects which two bimodulus material models have on strength predictions for graphite-epoxy composites. Nonlinear response of composite laminae are modeled in an approximate manner by employing piecewise linear and spline representations for transverse compression and shear stress-strain curves. The Tsai-Wu and Sandhu failure criteria are applied to predict failure of thin, laminated shells. The strength predictions are based on numerical solutions to Sanders' axisymmetric nonlinear shell equations. Numerical predictions for the strength and stress-strain response of internally pressurized rings are compared to experimental data cited from the literature.

I. Introduction

STRUCTURAL applications for laminates consisting of multiple layers of fiber-reinforced materials are currently increasing. Consequently, there exists a demand for precise mathematical modeling of composite material behavior. Certain fiber-reinforced materials exhibit different elastic behavior depending upon whether they are stressed in tension or compression. This behavior is commonly referred to as bimodulus behavior. The purpose of this paper is to present a strength analysis for thin, axisymmetric shells laminated of fibrous composites having nonlinear stress-strain and bimodulus material response.

Several mathematical models for bimodulus materials have been proposed.[1] The present study applies the analytical models developed by Ambartsumyan and Khachatryan[2] and Bert[3] to analyze the strength response of laminated shells. Most of the previous investigations of bimodulus structures have been directed at the static behavior of composite plates.[4-7] Recently, free vibration analyses of cross-ply laminated plates[8] and cylindrical shells[9] were considered.

Although the stress-strain behavior of bimodulus materials is nonlinear, it is usually modeled as being bilinear with different elastic moduli depending on the signs of the strains normal and transverse to the fiber direction. In this study, stress-strain responses for transverse compression and shear are modeled as being nonlinear, while all other stress-strain responses for an orthotropic composite are approximated as being linear. Two analytical strength criteria are used with these constitutive models to predict composite strengths. The strength criteria and material models have been incorporated into a finite difference computer program which can approximate the behavior of symmetrically loaded, axisymmetric composite shells.

II. Bimodulus Material Models and Failure Criteria

In order to present the effects that bimodulus materials have on the response of thin composite shells, a discussion of flat laminated plates will be considered first. Plate stiffnesses can be defined as

$$(A_{ij},B_{ij},D_{ij}) = \int_{-h/2}^{h/2} (1,z,z^2)\,(Q_{ij})\,(z)\,dz \qquad (i,j=1,2,6) \quad (1)$$

where h is the total plate thickness and z is measured from the plate midplane. The terms $Q_{ij}(z)$ are plane stress elastic stiffness defined as

$$\{\sigma_i\} = [Q_{ij}]\{\epsilon_j\} \qquad (i,j=1,2,6) \quad (2)$$

The definitions of in-plane, bending-extension, and bending or twisting coupling from Eq. (1) are used to form the constitutive equations for an arbitrary laminated plate. The constitutive equations can be written in partitioned form as

$$\begin{Bmatrix} N_i \\ \hline M_i \end{Bmatrix} = \left[\begin{array}{c|c} A_{ij} & B_{ij} \\ \hline B_{ij} & D_{ij} \end{array}\right] \begin{Bmatrix} \epsilon_j \\ \hline \kappa_j \end{Bmatrix} \qquad (i,j=1,2,6) \quad (3)$$

For laminates made of ordinary (non-bimodulus) materials, the elements of Q_{ij} are piecewise-constant functions of z. Laminate layers consist of unidirectional, fiber-reinforced material which is modeled as orthotropic with respect to its material symmetry axes: the fiber direction and two directions normal to it. When a single-layer plate or a plate symmetrically laminated about its midplane consists of ordinary materials, there is no coupling between stretching and bending (all B_{ij} terms vanish). Furthermore, when individual layers of a laminate are oriented parallel to the global plate axes, all A_{ij}, B_{ij}, and D_{ij} shear-normal coupling stiffnesses vanish.

However, a plate consisting of either a single bimodulus material layer or symmetrically laminated bimodulus material layers exhibits bending-stretching coupling. When a bimodulus plate is placed in bending, the differences in elastic moduli between tension and compression cause a shift in the neutral axis away from the compressive side of the bend if the compressive modulus is less than the tensile modulus. This bending-stretching coupling is analogous to an unsymmetrically laminated plate of ordinary orthotropic material. Consequently, for bimodulus materials, bending-stretching coupling can result from either bimodulus material response or laminate layup configuration. A listing of plate or shell stiffnesses that vanish for various laminate stacking sequences is presented in Table 1.

Received April 27, 1982; revision submitted Dec. 6, 1982.

*Staff Research Engineer, Engineering Mechanics Department.

The present study considers the effects that two bimodulus material models have on computed strengths of graphite-epoxy rings subjected to internal pressure. Because this type of loading does not produce significant bending response, elements of the stiffness matrices that are valid for ordinary materials are also valid for the bimodulus graphite-epoxy rings.

The first bimodulus material model employed for this study was proposed by Ambartsumyan and Khachatryan.[2] The compliances, S_{ij}, for this model are presented below with respect to the material symmetry directions of an orthotropic material in a state of plane principal stress.

When $\sigma_1 > 0$ and $\sigma_2 > 0$,

$$S_{11} = 1/E_1^t, \qquad S_{22} = 1/E_2^t$$
$$S_{12} = -\nu_{12}^t/E_1^t, \qquad S_{21} = -\nu_{21}^t/E_2^t \tag{4a}$$

When $\sigma_1 < 0$ and $\sigma_2 < 0$,

$$S_{11} = 1/E_1^c, \qquad S_{22} = 1/E_2^c$$
$$S_{12} = -\nu_{12}^c/E_1^c, \qquad S_{21} = -\nu_{21}^c/E_2^c \tag{4b}$$

When $\sigma_1 > 0$ and $\sigma_2 < 0$,

$$S_{11} = 1/E_1^t, \qquad S_{22} = 1/E_2^c$$
$$S_{12} = -\nu_{12}^t/E_1^t, \qquad S_{21} = -\nu_{21}^c/E_2^c \tag{4c}$$

When $\sigma_1 < 0$ and $\sigma_2 > 0$,

$$S_{11} = 1/E_1^c, \qquad S_{22} = 1/E_2^t$$
$$S_{12} = -\nu_{12}^c/E_1^c, \qquad S_{21} = -\nu_{21}^t/E_2^t \tag{4d}$$

where t and c denote tensile and compressive material properties, respectively.

The reciprocal relations that must be satisfied to guarantee symmetry of the compliance matrix are as follows:

$$\nu_{12}^t/E_1^t = \nu_{21}^t/E_2^t, \qquad \nu_{12}^c/E_1^c = \nu_{21}^c/E_2^c, \qquad \nu_{12}^t/E_1^t = \nu_{21}^c/E_2^c \tag{5}$$

From Eq. (5) it follows that the off-diagonal compliance elements are not affected by the sign of the principal stresses.

The second bimodulus model used for composite strength prediction was recently proposed by Bert.[3] Compliances for the Bert model are dependent on the sign of the stresses in the fiber direction, σ_f, and are as follows:

When $\sigma_f \geq 0$,

$$S_{11} = 1/E_1^t, \qquad S_{22} = 1/E_2^t$$
$$S_{12} = -\nu_{12}^t/E_1^t, \qquad S_{21} = -\nu_{21}^t/E_2^t \tag{6a}$$

When $\sigma_f < 0$,

$$S_{11} = 1/E_1^c, \qquad S_{22} = 1/E_2^c$$
$$S_{12} = -\nu_{12}^c/E_1^c, \qquad S_{21} = -\nu_{21}^c/E_2^c \tag{6b}$$

The reciprocal relations for the Bert model are the same as the first two relations listed in Eq. (5). Thus, Bert assumes that the compliance elements for tension and compression are independent.

The Tsai-Wu[10] and Sandhu[11] failure criteria have been used to compute laminate strengths. Two different formulations for the Tsai-Wu stress criterion have been employed. One formulation is based on the assumptiion of linear-elastic laminate response. Under this assumptiion, yield and ultimate stress in a lamina are analogous. However, an ultimate or failure state in one principal material coordinate direction does not necessarily lead to total lamina or laminate failure. Therefore, a second formulation employing the concept of stepwise reduction in laminae load-carrying capacity was developed. This concept was implemented by using bilinear

Table 1 Comparison of laminate stiffnesses for ordinary and bimodulus composite materials

Laminate type	Example laminate	Vanishing laminate stiffness: Ordinary material	Vanishing laminate stiffness: Bimodulus material
Aligned single or multiple-ply	0° or 90°/90°	$A_{16}, A_{26}, D_{16}, D_{26}$, All B_{ij}	$A_{16}, A_{26}, D_{16}, D_{26}$ B_{16}, B_{26}
Symmetrically balanced angle ply	30°/−30°/−30°/30°	A_{16}, A_{26}, All B_{ij}	None
$(0°/\pm\theta°)_s$	0°/+45°/−45°/−45°/+45°/0°	A_{16}, A_{26}, All B_{ij}	None

Table 2 Geometric parameters and bimodulus elastic material-property data for T300/5208 graphite-epoxy rings[14]

Ring geometric parameters		
Ply thickness, mm (in.)	0.132	(0.0052)
Ring thickness, mm (in.)	1.056	(0.0416)
Middle-surface radius, mm (in.)	50.8	(2.0)
Length, mm (in.)	25.4	(1.0)
Tension properties		
Fiber-direction Young's modulus, E_1, GPa (psi)	147.5	(21.4×10^6)
Transverse Young's modulus, E_2, GPa (psi)	9.3	(1.35×10^6)
Major Poisson's ratio, ν_{12}, dimensionless[a]	0.25	
In-plane shear modulus, G_{12}, GPa (psi)	5.72	(0.83×10^6)
Compression properties		
Fiber-direction Young's modulus, E_1, GPa (psi)	147.5	(21.5×10^6)
Transverse Young's modulus, E_2, GPa (psi)	14.3	(2.07×10^6)
Major Poisson's ratio, ν_{12}, dimensionless[a]	0.52	
In-plane shear modulus, G_{12}, GPa (psi)	5.72	(0.83×10^6)

[a] The minor Poisson's ratio is assumed to be given by the reciprocal relation.

approximations for nonlinear stress-strain curves corresponding to transverse compression and shear.

The Sandhu failure criterion differs from the Tsai-Wu criterion in the following respects: 1) ply failure is based on a strain energy formulation; 2) nonlinear stress-strain curves for transverse compression and shear are approximated by cubic spline functions; and 3) an equivalent, incremental-strain formulation is employed. Strain energies corresponding to laminae deformation parallel to the fiber direction, normal to the fiber direction, and in shear are assumed to be independent.

For this study, laminate failure predictions are based on either a first-ply-to-failure approach or a multiple-ply-to-failure approach. Multiple-ply predictions are based on the assumption that laminate failure occurs when fiber failure is predicted in at least two plies or when failure of two plies with different lamination orientations is predicted. After a laminate experiences first-ply failure, the degraded ply is assumed to unload under constant stress conditions. This assumption is appropriate since the ring specimens considered for this study were tested under load-controlled conditions.

III. Computed Strengths for Internally Pressurized Rings

Axisymmetric Shell Analysis

The bimodulus material models and failure criteria have been incorporated into a shell analysis based on Sanders' axisymmetric, nonlinear elastic shell theory.[12] These equations, combined with constitutive equations that account for general orthotropy of a laminated shell, can be expressed as six partial differential equations of first order in space and second order in time. These equations have the following matrix form:

$$Ix' + (\hat{G} + \tilde{G})x = f + M\ddot{x} \tag{7}$$

where x is a solution vector of six variables, I a 6×6 identity matrix, $\hat{G}$ and $\tilde{G}$ linear and nonlinear coefficient matrices of x, respectively, M a 6×6 mass matrix, and f a six-element load vector. Primes indicate spatial derivatives. The elements of $\hat{G}$, $\tilde{G}$, M, and f are listed in the Appendix.

A set of general boundary conditions for Eq. (7) at a shell edge can be written as

$$\Omega y + \Lambda z - l = 0 \tag{8}$$

where y and z are force and displacement subvectors of x, Ω and Λ 3×3 matrices, and l a 3×1 vector. The force and displacement subvectors are defined in the Appendix.

Equation (7) is converted into difference equations by utilizing central differences for the spatial derivatives and Houbolt backward differences for the time derivatives. The resulting system of nonlinear algebraic equations is solved by using an incremental Newton-Raphson algorithm.[13]

Comparisons of Computed Laminate Strengths to Available Experimental Data

In order to evaluate the effects which the bimodulus material models have on the accuracy of strength predictions for laminated composites, a set of experimental data was sought for comparison purposes. Data was found to be available from experiments conducted by Rowlands[14] on internally pressurized rings. The rings were constructed using a prepreg of Thornel (T-300) fibers in a 5208 resin matrix. The geometric parameters for the rings are listed in Table 2. The main advantage of ring specimens is that they are completely free of end constraints which can effect laminate strengths obtained from coupon specimens. Each ring specimen was instrumented with two three-element rosettes located diametrically opposite on the outside surface. The rings were loaded in pure hoop stress only by a hydrostatic testing device.

Rowlands also conducted experiments to characterize the basic material properties of the T-300/5208 material. Lamina properties evaluated include the tensile and compressive stress-strain response parallel and transverse to the fibers, and the in-plane shear stress-shear strain response. The longitudinal (0 deg) tensile response was obtained from 13×228 mm coupon specimens loaded through glass-epoxy tabs. The transverse (90 deg) tensile response was determined from 26×228 mm coupon specimens. The compression response of the graphite-epoxy material in the longitudinal and transverse directions were determined using 25-mm-wide

Table 3 Nondimensional failure stresses for $(0_2^\circ/\pm45^\circ)_s$ graphite-epoxy rings using the Tsai-Wu stress criterion[a]

Bimodulus material model	Laminate failure model	Stress criterion (linear model)	Stress criterion (bilinear model)	Experimental load	Laminate failure modes[b]
Ambartsumyan	Initial ply	1.871	2.296	2.150	Transverse tensile failure of 0° plies
	Multiple ply	2.128	2.322	2.150	Shear failure of ±45° plies
Bert	Initial ply	1.505	1.971	2.150	Transverse tensile failure of 0° plies
	Multiply ply	2.064	2.193	2.150	Shear failure of ±45° plies

[a] Nondimensional stresses computed from $N_h = \sigma_h r^2/E_1^t h^2$. [b] Numerically predicted failure modes identical to experimentally observed failure modes.

Table 4 Nondimensional failure stresses for $(0_2^\circ/\pm45^\circ)_s$ graphite-epoxy rings using the Sandhu strain energy criterion[a]

Bimodulus material model	Laminate failure model	Strain energy criterion	Experimental load	Laminate failure modes[b]
Ambartsumyan	Initial ply	2.010	2.150	Transverse tensile failure of 0° plies
	Multiple ply	2.816	2.150	Shear failure of ±45° plies
Bert	Initial ply	1.924	2.150	Transverse tensile failure of 0° plies
	Multiple ply	2.786	2.150	Shear failure of ±45° plies

[a] Nondimensional failure stresses computed from $N_j = \sigma_h r^2/E^t{}_1 h^2$. [b] Numerically predicted failure modes identical to experimentally observed failure modes.

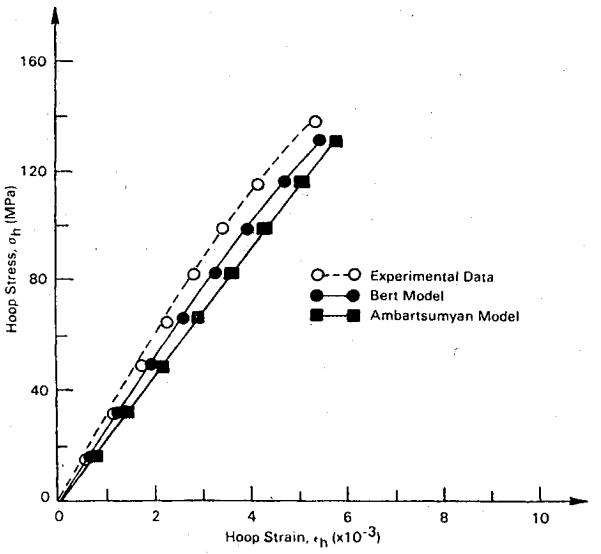

Fig. 1 Stress-strain response of $(0_2^\circ/\pm 45^\circ)_s$ ring using bilinear constitutive model.

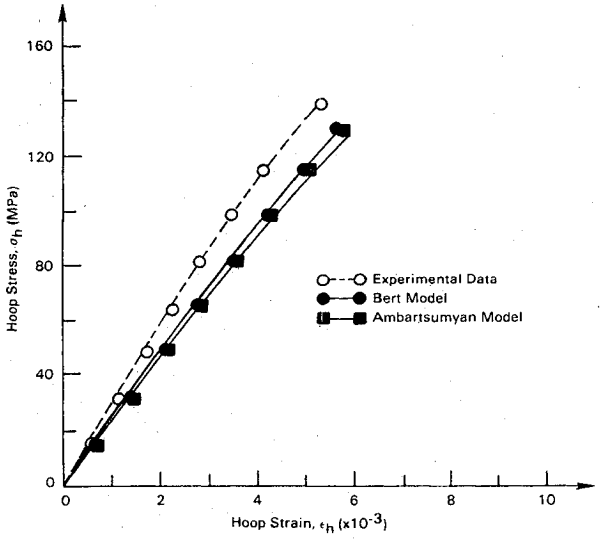

Fig. 2 Stress-strain response of $(0_2^\circ/\pm 45^\circ)_s$ ring using tangent modulus constitutive model.

sandwich beam specimens. The in-plane shear stress-strain lamina response was determined from ($\pm 45^\circ$) tensile coupons loaded through glass-epoxy tabs.[15] The elastic bimodulus material properties for the T300/5208 material are listed in Table 2.

Numerical predictions for failure stresses of the ring specimens have been completed for laminates with a $(0_2^\circ/\pm 45^\circ)_s$ layup configuration with respect to the ring axis. Comparisons between experimental and numerically predicted failure stress for the Tsai-Wu and Sandhu failure criteria are presented in Tables 3 and 4, respectively. Two numerical values for each bimodulus material model are listed. The first value corresponds to a first-ply failure strength prediction while the second value corresponds to a multiple-ply failure prediction. Comparisons between experimentally measured laminate hoop stresses and strains and numerically predicted midplane stresses and strains for the $(0_2^\circ/\pm 45^\circ)_s$ laminate are shown in Figs. 1 and 2. The strength results show that laminate failure stresses based on a multiple-ply failure approach generally overestimate the experimental failure loads. Therefore, all comparisons between strength predictions for the two bimodulus models are based on initial-ply failure. The failure mode sequence predicted by each criterion matches the experimentally observed failure sequence.

The stress and strain energy failure criteria predictions based on the Bert bimodulus model are shown in Tables 3 and 4 to be more conservative than the predictions based on the Ambartsumyan model. The numerical results also show the stress criterion to be more sensitive to the different bimodulus material formulations than the strain energy criterion. The stress criterion predictions varied by 17% between the two models, while the strain energy predictions varied by only 4%.

The sensitivities of the failure criteria to different bimodulus material models are also illustrated by the numerically predicted laminate stress-strain curves. The bilinear stress-strain approximation used with the stress criterion is shown in Fig. 1 to be sensitive to the two bimodulus material formulations. Stress-strain values predicted with the Bert model provide a closer approximation to the experimental data than those predicted with the Ambartsumyan model. The tangential stress-strain model used with the strain energy criterion is shown in Fig. 2 to be less sensitive to the two bimodulus material formulaitons.

IV. Summary and Conclusions

Fiber-reinforced composite materials are receiving increasing attention for structural applications because of their potential for weight savings. An important characteristic of many composite materials is that they exhibit different stiffnesses under compressive loading than under tensile loading. This material behavior is frequently referred to as bimodulus behavior. Isotropic bimodulus materials exhibit the characteristics of ordinary orthotropic materials. However, bimodulus orthotropic materials exhibit the response of ordinary anisotropic materials.

In the present paper, two mathematical models in the form of stress-strain relations are reviewed for bimodulus materials. The first model, as proposed by Ambartsumyan, employs compliance matrix elements which are dependent on the signs of principal stresses for a plane stress state. The second model, as proposed by Bert, employs independent compliance matrices which are dependent on the sign of stresses in the fiber direction. Effects which these two material models have on computed strengths of graphite-epoxy rings subjected to internal pressure have been determined for the Tsai-Wu and Sandhu failure criteria. Results of this study show that 1) laminate strength predictions based on the Bert model are more conservative than the predictions based on the Ambartsumyan model when compared to available experimental data; and 2) stress-strain curves predicted with the Bert model provide a closer approximation to experimental data than curves predicted with the Ambartsumyan model.

It should be noted that the strength predictions presented in this paper are based on a shell analysis which neglects the effects of transverse shear deformations. The thickness shear moduli of fiber-reinforced composites are generally an order of magnitude lower than their in-plane moduli. The shear modulus-elastic modulus ratio for isotropic materials is typically 40%. Thus, thin composite-material shells would be affected by thickness-shear flexibility to a greater degree than isotropic shells having the same geometrical dimensions. Future evaluations of orthotropic bimodulus material models using thin shell analysis should include the effects of transverse shear deformations.

Appendix: Definition of Matrix Elements

The axisymmetric shell equations in Eq. (7) are written with respect to the reference surface of a general shell of revolution shown in Fig. A1. The shell reference surface is defined by the coordinates ϕ and r. An arbitrary point within the shell may be defined by specifying the orthogonal coordinates, s, θ, and ζ, where s is the meridional coordinate, θ the circumferential coordinate, and ζ the normal coordinate originating at the shell reference surface. The principle radii of curvature are

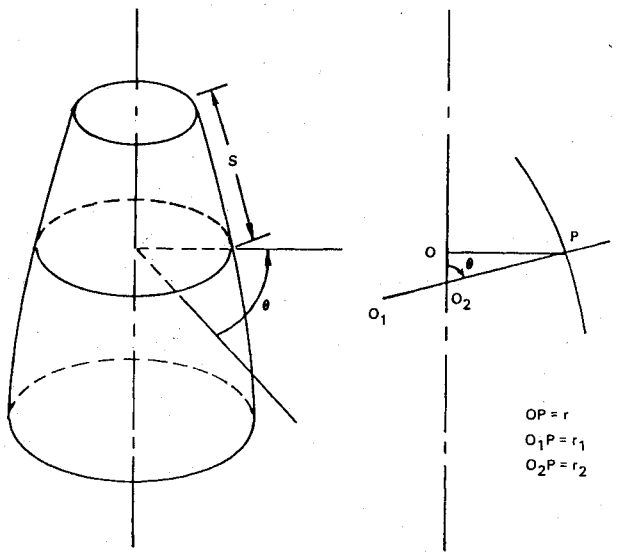

Fig. A1 Axisymmetric shell coordinates and radii of curvature.

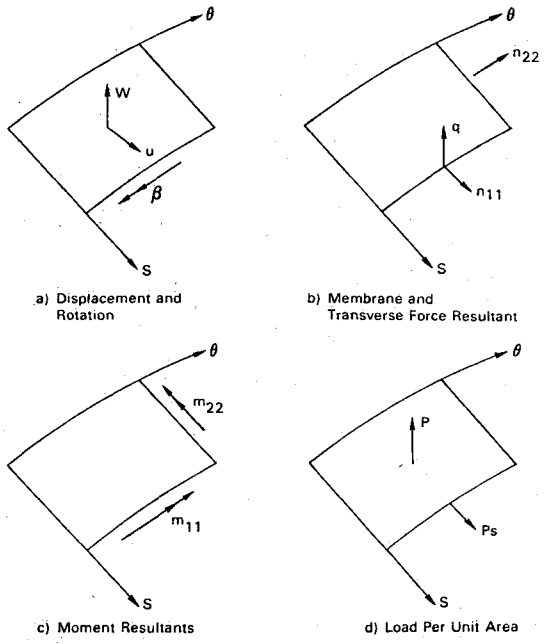

Fig. A2 Positive directions for displacements, rotations, membrane forces, moments and loads.

given by

$$1/r_1 = \phi' \tag{A1}$$

$$1/r_2 = \sin\phi/r \tag{A2}$$

where the prime denotes differentiation with respect to s.

The vector x of unknowns contained in Eq. (7) at a point is divided into two subvectors y_i and z_i

$$y_i = \begin{Bmatrix} n_{11} \\ q \\ m_{11} \end{Bmatrix}; \qquad z_i = \begin{Bmatrix} u \\ w \\ \beta \end{Bmatrix} \tag{A3}$$

where n_{11} and m_{11} are stress and bending moment results, respectively, q the shear resultant, u and w displacements, and β the meridional rotation. Positive directions for the shell unknowns and loads are shown in Fig. A2.

The nonzero elements of the 6×6 $\hat{G}$ matrix are

$$g_{11} = (\cos\phi/r)(1-N_{12}),\quad g_{12} = \phi'$$

$$g_{13} = -(\cos\phi/r)M_{12},\quad g_{14} = -(\cos^2\phi/r^2)(E_{12}+A_{12})$$

$$g_{15} = -(\cos\phi\sin\phi/r^2)(E_{12}+A_{22}),\quad g_{16} = (\cos^2\phi/r^2)(\hat{K}_{21}+B_{22})$$

$$g_{21} = -\phi' + (\sin\phi/r)N_{12},\quad g_{22} = \cos\phi/r$$

$$g_{23} = -(\sin\phi/r)M_{12},\quad g_{24} = -(\cos\phi\sin\phi/r^2)(E_{12}+A_{22})$$

$$g_{25} = -(\sin^2\phi/r^2)(E_{12}+A_{12}),\quad g_{26} = (\cos\phi\sin\phi/r^2)(\hat{K}_{21}+B_{22})$$

$$g_{31} = -(\cos\phi/r)N_3,\quad g_{32} = -1$$

$$g_{33} = (\cos\phi/r)(1-M_3),\quad g_{34} = -(\cos^2\phi/r^2)(E_3+B_{22})$$

$$g_{35} = -(\cos\phi\sin\phi/r^2)(E_3+B_{22}),\quad g_{36} = (\cos^2\phi/r^2)(K_3+D_{22})$$

$$g_{41} = -D_{11}/G,\quad h_{42} = 0$$

$$g_{43} = B_{11}/6,\quad g_{44} = (\cos\phi/r)N_{12}$$

$$g_{45} = \phi' + N_{12}(\sin\phi/r),\quad g_{46} = -(\cos\phi/r)N_3$$

$$g_{51} = g_{52} = g_{53} = g_{55} = 0,\quad g_{54} = -\phi'$$

$$g_{56} = -1,\quad g_{61} = -(B_{11}/G)$$

$$g_{62} = 0,\quad g_{63} = A_{11}/G$$

$$g_{64} = -(\cos\phi/r)M_{12},\quad g_{65} = -(\sin\phi/r)M_{12}$$

$$g_{66} = (\cos\phi/r)M_3 \tag{A4}$$

The constant terms in Eqs. (A4) are:

$$G = A_{11}D_{11} - B_{11}^2$$

$$N_{12} = (1/G)(A_{12}D_{11} - B_{11}B_{12})$$

$$M_{12} = (1/G)(A_{11}B_{12} - A_{12}B_{12})$$

$$E_{12} = (1/G)(2A_{12}B_{11}B_{12} - A_{12}^2D_{11} - A_{11}B_{12}^2)$$

$$\hat{K}_{21} = (1/G)(A_{12}D_{12}B_{11} - A_{12}D_{11}B_{12} + B_{11}B_{12}^2 - A_{11}D_{12}B_{12})$$

$$N_3 = (1/G)(D_{11}B_{12} - D_{12}B_{11})$$

$$M_3 = (1/G)(A_{11}D_{12} - B_{11}B_{12})$$

$$E_3 = \hat{K}_{21}$$

$$K_3 = (1/G)(2D_{12}B_{11}B_{12} - D_{11}B_{12}^2 - A_{11}D_{12}^2) \tag{A5}$$

The A_{ij}, B_{ij}, and D_{ij} constants arise from the orthotropic constitutive relations

$$\begin{Bmatrix} n_{11} \\ n_{22} \\ m_{11} \\ m_{22} \end{Bmatrix} = \begin{bmatrix} A_{11} & A_{12} & B_{11} & B_{12} \\ A_{12} & A_{22} & B_{12} & B_{22} \\ B_{11} & B_{12} & D_{11} & D_{12} \\ B_{12} & B_{22} & D_{12} & D_{22} \end{bmatrix} \begin{Bmatrix} e_{11} \\ e_{12} \\ \kappa_{11} \\ \kappa_{22} \end{Bmatrix} \tag{A6}$$

In Eq. (A6) n_{ij} and m_{ij} are the force and moment resultants defined in Fig. A2, and e_{ij} and κ_{ij} are tensor strains and curvatures. The nonzero elements of the 6×6 $\tilde{G}$ matrix are

$$\tilde{g}_{11}=\phi'\beta \qquad \tilde{g}_{26}=n'_{11}$$

$$\tilde{g}_{21}=(\cos\phi/r)\beta+\beta' \qquad \tilde{g}_{46}=\beta/2 \qquad \text{(A7)}$$

The nonzero elements of the six-element f vector are

$$f_1=-p_s, \qquad f_2=-p \qquad \text{(A8)}$$

The nonzero elements of the 6×6 M matrix are

$$M_{14}=M_{25}=1 \qquad \text{(A9)}$$

References

[1]Bert, C. W., "Recent Advances in Mathematical Modeling of the Mechanics of Bimodulus, Fiber-Reinforced Composite Materials," *Proceedings of the 15th Annual Meeting, Society of Engineering Science*, Gainesville, Fla., 1978, pp. 101-106.

[2]Ambartsumyan, S. A. and Khachatryan, A. A., "The Basic Equations of the Theory of Elasticity for Materials with Different Tensile and Compressive Strengths (Stiffnesses)," *Mechanics of Solids*, Vol. 1, Jan. 1966, pp. 29-34.

[3]Bert, C. W., "Models for Fibrous Composites with Different Properties in Tension and Compression," *Journal of Engineering Materials and Technology*, Vol. 99H, Oct. 1977, pp. 344-349.

[4]Jones, R. M. and Morgan, H. S., "Bending and Extension of Cross-Ply Laminates with Different Moduli in Tension and Compression," *Computers and Structures*, Vol. 11, March 1980, pp. 181-190.

[5]Kincannon, S. K., Bert, C. W., and Sudhakar Reddy, V., "Cross-Ply Elliptic Plates of Bimodulus Material," *Journal of the Structural Division, Proceedings of the ASCE*, Vol. 106, July 1980, pp. 1437-1449.

[6]Reddy, J. N. and Chao, W. C., "Finite-Element Analysis of Laminated Bimodulus Plates," *Computers and Structures*, Vol. 12, No. 2, 1980, pp. 245-251.

[7]Bert, C. W., Reddy, J. N., Sudhakar Reddy, V., and Chao, W. C., "Bending of Thick Rectangular Plates Laminated of Bimodulus Composite Materials," *AIAA Journal*, Vol. 19, Oct. 1981, pp. 1342-1349.

[8]Bert, C. W., Reddy, J. N., Chao, W. C., and Reddy, V. S., "Vibrations of Thick Rectangular Plates of Bimodulus Composite Material," *Journal of Applied Mechanics*, Vol. 48, June 1981, pp. 371-376.

[9]Bert, C. W. and Kumar, M., "Vibration of Cylindrical Shells of Bimodulus Composite Materials," *Journal of Sound and Vibration*, Vol. 81, March 1982, pp. 107-121.

[10]Tsai, S. W. and Wu, E. M., "A General Theory of Strength for Anisotropic Materials," *Journal of Composite Materials*, Vol. 5, Jan. 1971, pp. 58-80.

[11]Sandhu, R. S., "Nonlinear Response of Unidirectional and Angle-Ply Laminates," *Journal of Aircraft*, Vol. 13, Feb. 1976, pp. 104-111.

[12]Sanders, J. L. Jr., "Nonlinear Theories for Thin Shells," *Quarterly of Applied Mathematics*, Vol. 23, Jan. 1963, pp. 21-36.

[13]Stephens, W. B. and Fulton, R. E., "Axisymmetric Static and Dynamic Buckling of Spherical Caps Due to Centrally Distributed Pressures," *AIAA Journal*, Vol. 11, Nov. 1969, pp. 2120-2126.

[14]Rowlands, R. E., "Analytical-Experimental Correlatin of the Biaxial State of Stress in Composite Laminates," Wright Patterson AFB, Ohio, AFFDL-TR-75-11, April 1975.

[15]Petit, P. H., "A Simplified Method of Determining the Inplane Shear Stress-Strain Response of Unidirectional Composites," *Composite Materials: Testing and Design, ASTM STP 460*, American Society of Testing and Materials, 1969, pp. 83-92.